AIAA JOURNAL
Vol. 40, No. 9, September 2002

Numerical Simulation of Sonic Boom Focusing

Thierry Auger*
Airbus France SAS, 31060 Toulouse Cedex 03, France
and
François Coulouvrat†
Centre National de la Recherche Scientifique, 75015 Paris, France

A numerical method is presented to simulate the focusing of sonic booms. In the vicinity of caustics, the pressure satisfies the nonlinear Tricomi equation. To solve this equation, an iterative algorithm, based on an unsteady version of the equation, is used. The algorithm is a modification of the pseudospectral code used for solving the Zabolotskaya–Khokhlov (KZ) equation. In the linear case, the code is validated by comparison with analytical solutions. For an incoming *N* wave, the shape of the outgoing wave observed in flight tests is recovered. In the nonlinear case, no analytical solution is known to compare with the numerical output. Validation of the numerical scheme is completed by means of four different tests. First, comparisons with the linear case shows that the numerical solutions behave as expected from the physics. Second, the solution after convergence is proved to be independent of the initial guess. Third, the maximal signal amplitude is proved to converge while increasing the discretization. Finally, the numerical scheme is checked against the nonlinear Guiraud's scaling law. In the last part, an application to the focusing of Concorde sonic boom in acceleration is presented, and ways of reducing focused booms are discussed.

Nomenclature

Ai	=	Airy function
$A(\omega)$	=	matrix resulting from finite differences discretization of the linear Tricomi equation in the frequency domain
$\boldsymbol{B}$	=	vector resulting from finite differences discretization of the linear Tricomi equation in the frequency domain
C_G	=	Guiraud's scaling law[1] constant for acoustic pressure
C_{Gz}	=	Guiraud's scaling law[1] constant for distance to the caustic
$C_{G\tau}$	=	Guiraud's scaling law[1] constant for phase variable
$c_{\text{nonlinear}}$	=	nonlinear sound velocity
c_0	=	ambient sound speed at rest
$\bar{F}$	=	dimensionless incoming wave
f	=	amplification coefficient
$\bar{G}$	=	dimensionless outgoing wave
M_{ac}	=	acoustic Mach number
P_{ac}	=	magnitude order of incoming acoustic pressure
$\hat{P}$	=	Fourier transform of dimensionless acoustic pressure
p	=	thermodynamic pressure of the fluid
p_a	=	acoustic pressure
$\bar{p}_a$	=	dimensionless acoustic pressure
$\bar{p}_a^{\max}$	=	maximum amplitude of dimensionless acoustic pressure
p_0	=	ambient pressure at rest
R_{cau}	=	relative radius, $1/(1/R_{\text{sec}} - 1/R_{\text{ray}})$
R_{ray}	=	radius of curvature of the projection in the plane (Oxz) of the ray tangent to the caustic
R_{sec}	=	radius of curvature of the intersection of the caustic surface with the plane (Oxz)
T_{ac}	=	characteristic duration of the incoming acoustic signal
t	=	time variable
$\bar{t}$	=	pseudotime variable
Z	=	dimensionless distance (Guiraud's scaling[1])
z	=	distance to the caustic
$\bar{z}$	=	dimensionless distance to the caustic
β	=	nonlinearity parameter of the medium
γ	=	ratio of specific heats
δ	=	characteristic thickness of the diffraction boundary layer around the caustic
Θ	=	dimensionless phase variable (Guiraud's scaling[1])
μ	=	measurement of nonlinear effects relative to diffraction
Π	=	dimensionless pressure (Guiraud's scaling[1])
ρ_0	=	ambient density at rest
$\bar{\tau}$	=	dimensionless phase variable
ω	=	pulsation

I. Introduction

INASMUCH as sonic booms remain a community acceptance problem, the development of future civil supersonic aircraft (either supersonic transport or business jet) may be threatened by supersonic operations restricted to overwater routes only. Sonic boom focusing occurs during certain maneuvers, leading to amplification of ground pressures up to 2–5 times the carpet boom shock strength. Such levels are likely to be banned by a future international regulation on sonic boom. Operating conditions may prevent certain maneuvers (sharp turns and sonic cutoff at low Mach flight numbers) producing sonic boom focusing. However, the focusing resulting from transonic acceleration from Mach 1 to cruise speed cannot be avoided by realistic maneuvers. Therefore, future supersonic civil aircraft will have to satisfy acceptable levels of focused booms.

According to classical theory,[1,2] sonic booms are computed within the framework of geometrical acoustics. The eikonal (phase) function is determined by the ray path and the signal amplitude by the ray-tube area. Nonlinear effects along each ray explain the pressure signal distortion from the complicated shock flow around the aircraft body down to the simple N wave at ground level. Caustics are surfaces (and their ground intersection are lines) where the ray-tube area vanishes; geometrical acoustics becomes singular there

Received 3 July 2001; revision received 27 February 2002; accepted for publication 1 March 2002.

*Engineer, EEA M0132/7, 316 route de Bayonne; thierry.auger@airbus.com.

†Researcher, Laboratoire de Modélisation en Mécanique, Université Pierre et Marie Curie, 8 rue du capitaine Scott; coulouvr@ccr.jussieu.fr.

because it neglects diffraction (acoustic velocity in the wavefront plane). This approximation breaks down near caustics. Around regular smooth caustics surfaces (fold caustics according to the terminology of catastrophe theory[3]), diffraction at first order can be recovered in the linear case by considering a diffraction boundary layer around the caustic.[4] There, the pressure can be shown to satisfy the linear Tricomi equation; its intrinsic solution is the well-known Airy function, in agreement with catastrophe theory. If the incoming signal possesses shock waves as for sonic boom N waves, the amplified signal near the caustics and the outgoing signal exhibit a U shape resulting from the $\pi/2$ phase jump through the caustics. This shape is substantiated by measurements,[5] but a linear theory would predict infinite peaks for the U wave. To recover finite signals, it is necessary to take into account nonlinearities as an additional limiting mechanism. Indeed, because nonlinearities induce the shock waves responsible for the singular peaks of the U wave during propagation, it is consistent that they must also be taken into account at focusing where the signal reaches its highest amplitude. The resulting equation is the so-called nonlinear Tricomi equation (see Ref. 1), which is a mixed-type (elliptical/hyperbolic) equation. The process of linear diffraction being the dominant mechanism around caustics, supplemented by nonlinearities, is supported by laboratory-scale experiments[6] at small Mach numbers. The objective of this paper is to present a numerical method for solving the nonlinear Tricomi equation using a pseudospectral method.

Since the early 1970s, several techniques have been elaborated for solving the nonlinear Tricomi equation. Seebass[7] and Gill and Seebass[8] recover the linear Tricomi equation using a hodograph transform. The main drawback is that boundary conditions are transposed directly into the hodograph space without transformation, so that they cannot be satisfied exactly. The advantage is that the problem in the hodograph space is fully linear and can be solved analytically. Returning from hodograph variables to physical ones yields gaps or multivalued profiles. This difficulty is overcome by introducing shocks or expansion fans. Because shock conditions cannot be satisfied simultaneously for both pressure and transverse velocity, the position of shock waves is determined approximately. Finally, the method is practically limited to the weakest amplitude signals. For higher amplitudes, Guiraud's scaling law[1] has to be used, although it is theoretically restricted to step shocks only. Otherwise, direct numerical simulations of the nonlinear Tricomi equation were undertaken using finite differences. Seebass et al.[9] implemented a shock-capturing scheme by applying the switch developed by Murman and Cole[10] to simulate transonic flows. The numerical scheme is stable and convergent, but the numerical viscosity introduced to stabilize solutions reduces the peak amplitude of the U wave in an uncontrolled way. A shock-fitting solver was developed by Yu and Seebass[11] based on the method of Moretti.[12] Position and amplitude of shocks are fairly accurate, but the method is rather intricate, and the process is not unconditionally stable. McDonald and Kuperman[13] simulate the focusing of weak acoustic shock waves by means of the nonlinear progressive wave equation. This is a nonlinear version of the parabolic approximation, similar to the Khokhlov and Zabolotskaya[14] (KZ) equation, but its evolution is in time instead of space. By this method, focusing is simulated directly as a result of propagation in an inhomogeneous medium and does not require the local resolution of the nonlinear Tricomi equation. Their[13] observations are in qualitative agreement with the nonlinear Tricomi equation (formation of peaks, displacement of the maximum overpressure), but no detailed investigations or comparisons have been performed.

None of the numerical methods presented can be considered fully validated and, therefore, completely reliable. Indeed, no validations have been made in the linear case with analytical solutions (except the method of hodograph transform, which is in a way an astute linearization), no test of convergence have been presented, and validations of the fully nonlinear code by checking the nonlinear Guiraud's scaling law[1] are lacking. Consequently, the method of the hodograph, despite its limitations, remains until now the only method used for evaluating sonic boom focusing.[15] Moreover, although accepted in the sonic boom community, the Tricomi nonlinear equation still remains to be proved as a validated model for describing sonic boom focusing, by quantitative (and no more qualitative) comparisons with measurements (either test flights or laboratory-scale experiments). Because only approximate solutions of the nonlinear Tricomi equations are available, a fully validated numerical code appears to be an indispensable tool to reach that ultimate goal. The objective of this paper to is present a new numerical solver (Sec. III) of the nonlinear Tricomi equation (Sec. II), fully validated both in the linear (Sec. IV) and nonlinear (Sec. V) cases. Finally, this solver will be used to evaluate the focusing of the Concorde sonic boom during its acceleration phase, and potential ways for reducing focused sonic booms will be briefly indicated (Sec. VI).

II. Theory

The derivation of the nonlinear Tricomi equation in a two- or three-dimensional, quiescent, inhomogeneous fluid can be found in several references[1,16–18] and is not reproduced here. Its generalization to a heterogeneous fluid with stationary flow can be found in Ref. 19.

A caustic is an envelope surface of rays. At a point near a caustic surface, there are either two rays (one incoming ray going through the point before intersecting the caustic tangentially, and one outgoing ray going through the point after having intersected the caustic tangentially) or zero (shadow zone), depending on which side of the caustic the point is (Fig. 1). Near point O located on the caustic, we introduce the Cartesian coordinate system $(Oxyz)$ with O–x the axis in the plane tangent to the caustic and oriented along the ray tangent to the caustic at point O and O–z the axis in the direction normal to the caustic, away from the shadow zone, and O–y the third direction. We note the ambient density ρ_0, the ambient sound speed c_0, and the ambient pressure p_0 at point O. The acoustic pressure field is $p_a(x, y, z, t)$. The local caustic geometry is determined by R_{sec}, the radius of curvature of the intersection of the caustic surface with the plane (Oxz), R_{ray}, the radius of curvature of the projection in the plane (Oxz) of the ray tangent to the caustic at point O, and $R_{\text{cau}} = 1/(1/R_{\text{sec}} - 1/R_{\text{ray}})$, the relative radius (Fig. 1).

We assume the incoming signal near point O at a distance δ (defined later) from the caustic has a characteristic duration T_{ac}, a maximum overpressure P_{ac}, and a related acoustical Mach number $M_{\text{ac}} = P_{\text{ac}}/\rho_0 c_0^2$. With air the carrier fluid, the nonlinearity parameter of the medium is $\beta = (1+\gamma)/2 = 1.2$. In dimensionless variables, the nonlinear Tricomi equation for the dimensionless acoustic pressure $\bar{p}_a = (p - p_0)/P_{\text{ac}}$ is[19]

$$\frac{\partial^2 \bar{p}_a}{\partial \bar{z}^2} - \bar{z}\frac{\partial^2 \bar{p}_a}{\partial \bar{\tau}^2} + \mu \frac{\partial^2}{\partial \bar{\tau}^2}\left(\frac{\bar{p}_a^2}{2}\right) = 0 \tag{1}$$

with the dimensionless phase variable

$$\bar{\tau} = [t - x(1 - z/R_{\text{sec}})/c_0]/T_{\text{ac}} \tag{2}$$

and the dimensionless distance to the caustic

$$\bar{z} = \left[2/\left(c_0^2 T_{\text{ac}}^2 R_{\text{cau}}\right)\right]^{\frac{1}{3}} z = z/\delta \tag{3}$$

where

$$\mu = 2\beta M_{\text{ac}}[R_{\text{cau}}/(2c_0 T_{\text{ac}})]^{\frac{2}{3}} \tag{4}$$

Here δ is the characteristic thickness of the diffraction boundary layer around the caustic in which diffraction effects cannot be neglected. Physically, it is defined as the distance at which the phases of

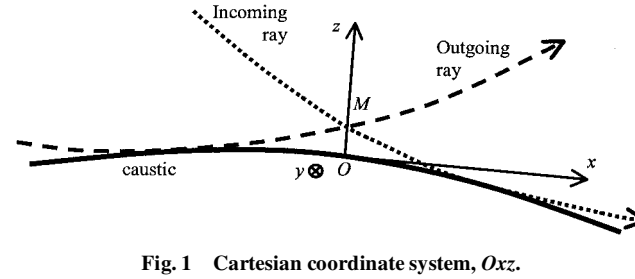

Fig. 1 Cartesian coordinate system, *Oxz*.

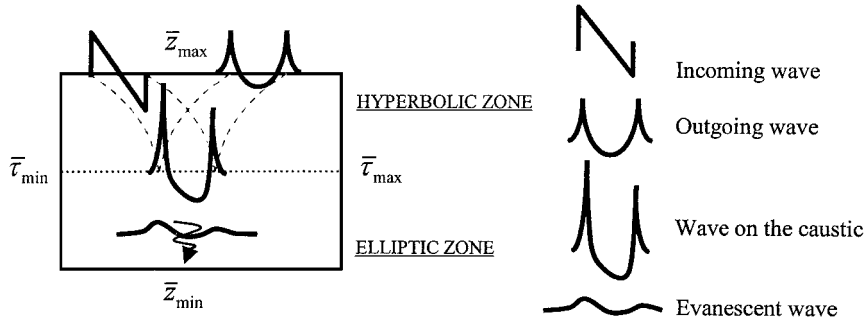

Fig. 2 Boundary conditions and computational domain for an incoming N wave.

incoming and outgoing signals differ from less than T_{ac}. The parameter μ is a measurement of nonlinear effects relative to diffraction. For sonic booms, it is generally small, of order 0.1 (see Sec. VI). The assumption that the pressure field is supposed to depend at first order only on the two variables $\bar{\tau}$ and $\bar{z}$ instead of the four physical ones t, x, y, and z is in agreement with the theory of catastrophes for fold caustics.

The boundary conditions are given as follows (Fig. 2). At large times, the signal vanishes:

$$\bar{p}_a(\bar{\tau} \to \pm\infty, \bar{z}) = 0 \tag{5}$$

Far into the shadow zone, by using asymptotic expansion of Airy function[20] for larger $\bar{z}$ that are solutions of the linear Tricomi equation in the frequency domain [see Eq. (10)]:

$$Ai(-\bar{z}) \sim \left(1/2\sqrt{\pi}\right)\bar{z}^{-\frac{1}{4}} \exp\left(-\tfrac{2}{3}\bar{z}^{\frac{3}{2}}\right)$$

The signal vanishes exponentially (evanescent wave):

$$\bar{p}_a(\bar{\tau}, \bar{z} \to -\infty) = 0 \tag{6}$$

Far away from the caustic, the matching with geometrical acoustics implies that the signal splits into an incoming wave $\bar{F}$ and an outgoing wave $\bar{G}$ as follows:

$$\bar{p}_a(\bar{\tau}, \bar{z} \to +\infty) \sim \bar{z}^{-\frac{1}{4}}\left[\bar{F}\left(\bar{\tau} + 2\bar{z}^{\frac{3}{2}}/3\right) + \bar{G}\left(\bar{\tau} - 2\bar{z}^{\frac{3}{2}}/3\right)\right] \tag{7}$$

where only the incoming wave is explicitly known (determined by geometrical acoustics), with the outgoing one being dependent on $\bar{F}$ and μ. The amplitude dependence $\bar{z}^{-1/4}$ illustrates that geometrical acoustics is singular near caustics. The outgoing wave $\bar{G}$ can be eliminated by rewriting Eq. (7) under the form of a radiation condition:

$$\bar{z}^{\frac{1}{4}}\frac{\partial \bar{p}_a}{\partial \bar{\tau}} + \bar{z}^{-\frac{1}{4}}\frac{\partial \bar{p}_a}{\partial \bar{z}} = 2\frac{\mathrm{d}\bar{F}}{\mathrm{d}\bar{\tau}}\left(\bar{\tau} + \frac{2}{3}\bar{z}^{\frac{3}{2}}\right) \tag{8}$$

Note that the nonlinear Tricomi equation is a mixed hyperbolic/elliptic type, depending on the sign of $z - \mu \bar{p}^a$, which models the continuous transition from geometrical acoustics (hyperbolic zone insonified by acoustical rays) to the shadow (elliptical) zone.

III. Numerical Algorithm

To solve the nonlinear Tricomi equation (1) with boundary conditions Eqs. (5), (6), and (8), an iterative algorithm based on an unsteady version of the equation is used:

$$\frac{\partial^2 \bar{p}_a}{\partial \bar{t}\,\partial \bar{\tau}} = \frac{\partial^2 \bar{p}_a}{\partial \bar{z}^2} - \bar{z}\frac{\partial^2 \bar{p}_a}{\partial \bar{\tau}^2} + \mu\frac{\partial^2}{\partial \bar{\tau}^2}\left(\frac{\bar{p}_a^2}{2}\right) \tag{9}$$

with an artificial pseudotime variable $\bar{t}$.

The idea of solving steady problems as large time limits of unsteady ones is rather common in computational fluid dynamics (CFD) and has been especially successful in transonic aerodynamic computations. The arbitrary choice of the additional term on the left-hand side of Eq. (9) is motivated by analogy with similar equations

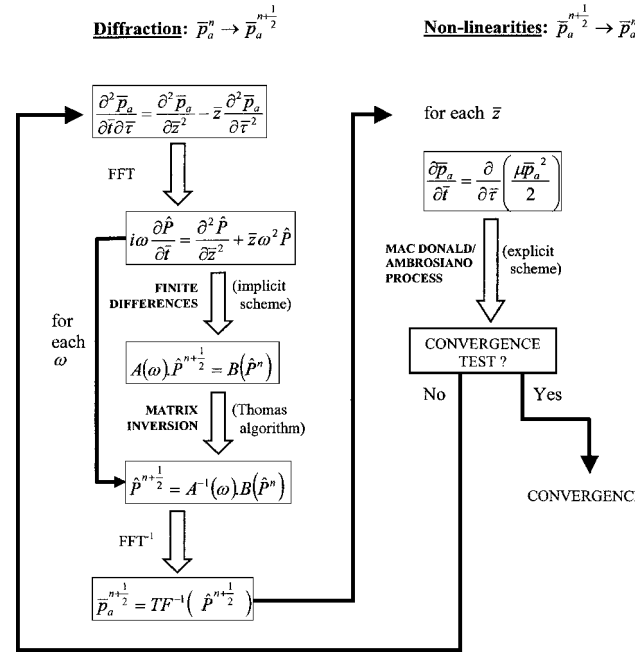

Fig. 3 Details of numerical algorithm.

describing coupled nonlinear and diffraction effects in acoustics, such as the KZ equation modeling finite amplitude sound beams[14] or pressure field near caustics cusps[21] or the nonlinear propagation of sonic booms beyond the carpet cutoff.[22] Equation (9) reduces to the inviscid KZ equation by omitting the term proportional to $\bar{z}$. The numerical algorithm for solving Eq. (9) is based on a modification of a pseudospectral code used for solving the KZ equation.[23] Its structure is shown in the Fig. 3. Each iteration in pseudotime $\bar{t}$, $\bar{p}_a^n(\bar{\tau}, \tau\bar{z}) = \bar{p}_a(\bar{t} = n\Delta\bar{t}, \bar{\tau}, \tau\bar{z})$, is split into two substeps: In the first one, $\bar{p}_a^n \to \bar{p}_a^{n+1/2}$, nonlinear terms are omitted, and diffraction is treated in the frequency domain after a fast Fourier transform (FFT), $\hat{P}(\bar{t}, \omega, \bar{z}) = \mathrm{FFT}\,[\bar{p}_a(\bar{t}, \bar{\tau}, \bar{z})]$. For each frequency ω, the second derivative in $\bar{z}$ is discretized by an implicit second-order, centered finite difference, and the first derivative in $\bar{t}$ is discretized by a first-order finite difference. Boundary conditions are discretized in the frequency domain by noncentered finite differences at second order for matching with geometrical acoustics, and at first order in the shadow zone. The resulting matrix systems $A(\omega) \cdot \hat{P}^{n+1/2} = \boldsymbol{B}(\omega, \hat{P}^n)$ are inverted for each frequency by a standard algorithm for a tridiagonal matrix. Then we return by an inverse FFT into the physical space. In the second substep $\bar{p}_a^{n+1/2} \to \bar{p}_a^n$, diffraction is omitted. Equation (9) reduces to a series of inviscid Burgers's equations[24] for each $\bar{z}$ value, which are solved using the total variation diminishing shock-capturing numerical scheme of McDonald and Ambrosiano.[24] The Courant–Friedrichs–Lewy condition for the McDonald and Ambrosiano scheme[24] imposes the largest possible step $\Delta\bar{t}$ for the pseudotime. Finally, these two successive steps are repeated until convergence. Numerical convergence is obtained when the maximum deviation between two

successive iterations is less than a prescribed value. Details on the numerical scheme can be found in Ref. 19. Computations have been performed for an incoming N wave, characteristic of sonic boom signal on the ground. The computational domain is shown in Fig. 1. Unless otherwise specified, simulations are performed for an incoming N wave with 3500 points in the $\bar{z}$ direction and 1024 frequencies associated to the phase variable $\bar{\tau}$. The computational domain for an N wave is ($\bar{z} \in [-1; 1]$ and $\bar{\tau} \in [-8/3; 11/3]$).

IV. Validation of Numerical Scheme in Linear Case

Validation in the linear case is especially important because the linear solution exhibits sharp peaks specific to this acoustical problem. (No equivalent is known in transonic aerodynamics.) A validated numerical scheme must prove its ability to capture the peaks numerically. The convergence of the numerical scheme has been studied by comparison with the analytical solutions expressed as Fourier transforms (TF) of the Airy function (Gill and Seebass[8]):

$$\bar{p}_a(\bar{\tau}, \bar{z}) = \sqrt{2\pi}\,\mathrm{TF}^{-1}\left\{\mathrm{TF}(F)(\omega)[1 + i\,\mathrm{sgn}(\omega)]|\omega|^{\frac{1}{6}} Ai\left(-|\omega|^{\frac{2}{3}}\bar{z}\right)\right\} \tag{10}$$

The initial guess for initiating the iterative algorithm is the zero function. As shown in Fig. 4, at five distances from the caustic, the numerical (solid line) and analytical (broken line) solutions perfectly superimpose; the scheme is entirely validated in the linear case. That the peaks have a finite amplitude is due to the finite range after discrete FT of the frequency spectrum of both the analytical or numerical solutions.

Moreover, Fig. 4 shows the evolution of the pressure waveforms while approaching the caustic. At $\bar{z} = 1.5$, we recognize the incoming N wave and the outgoing U wave (in the linear case, the Hilbert transform of the incoming wave). At $\bar{z} = 1$, the two signals begin to intermix. On the caustic, $\bar{z} = 0$, the characteristic asymmetric U wave reaches its maximum singularity at sharp peaks. In the shadow zone, $\bar{z} = -0.5$, the peaks fade out dramatically into a smooth profile decaying with distance. This well-known behavior is strongly corroborated by results from flight tests.[5] However, the time discretization hides the infinite peaks associated with the linear case. This is one of the difficulties in developing a numerical code in the nonlinear case: Any stable scheme (for instance, by introducing frequency filtering or numerical viscosity) will lead to good looking pressure waveforms with finite amplitudes. However, confidence in the solver can be achieved only if it is proved that nonlinearities are taken into account in a proper way. A careful validation of the nonlinear algorithm is the objective of the next section.

V. Validation of Numerical Scheme in Nonlinear Case

In the nonlinear case, no analytical solution is known with which to compare the numerical output. Validation is ensured through four different tests. First, comparisons with the linear case will show that the numerical solutions behave as expected from the physics. Second, the solution after convergence will be proved to be independent of the initial guess. Third, the maximal signal amplitude will be proved to converge while increasing the discretization. Finally, the numerical scheme will be checked against the nonlinear Guiraud's scaling law.[1]

In Fig. 5, linear (broken line) and nonlinear ($\mu = 0.08$) (solid line) results are shown. There are two noticeable features associated with nonlinear effects. First, nonlinearities decrease the amplitude of the signal by dissipating part of the energy of the sharp peaks into shock waves. The amplitude decrease is especially dramatic on the caustic. Second, the bow peak is in advance compared to its linear counterpart. This is due to the nonlinear sound velocity $c_{\mathrm{nonlinear}} = c_0 + \beta P_{\mathrm{ac}}/\rho_0 c_0$, which accelerates higher pressures relatively to lower ones. This effect is much less pronounced for the tail peak that follows an expansion wave slowed down by nonlinearities.

Figure 6 shows the pressure gray plot (dark values corresponding to the highest pressure levels) of the entire numerical domain, in both the linear and nonlinear cases ($\mu = 0.08$). For each case, we clearly see the hyperbolic and the elliptical domains and, in the former, the characteristic curves associated to the bow and tail ingoing (outgoing) shocks (peaks). As noted earlier, the characteristic curves associated to the bow shock undergo more deformations. The two domains are separated by the geometrical caustic ($\bar{z} = 0$) in the linear case and by the sonic line ($\bar{z} = \mu \bar{p}_a$, black line, Fig. 6) in the nonlinear one. The points of maximum pressure indicated by the circles are moved away from the caustic. In the nonlinear case, the maximum amplitude is no longer on the geometrical caustics. These points of maximum amplification are extremely close to the sonic line, but a more detailed study of the numerical results indicate that they are located slightly below the sonic line, inside the elliptical domain. All three nonlinear features (amplitude decrease, phase shifting of bow peaks, and displacement of points of maximum amplitude below the sonic line) are amplified with the increase of the nonlinear coefficient μ.

The next validation is presented in Fig. 7, showing the computed time signals at the caustic (solid line) found from four very different initial guesses [broken line, zero (Fig. 7a), linear solution (Fig. 7b), opposite of the linear solution (Fig. 7c), and crenel (Fig. 7d)]. The four solutions after convergence are perfectly

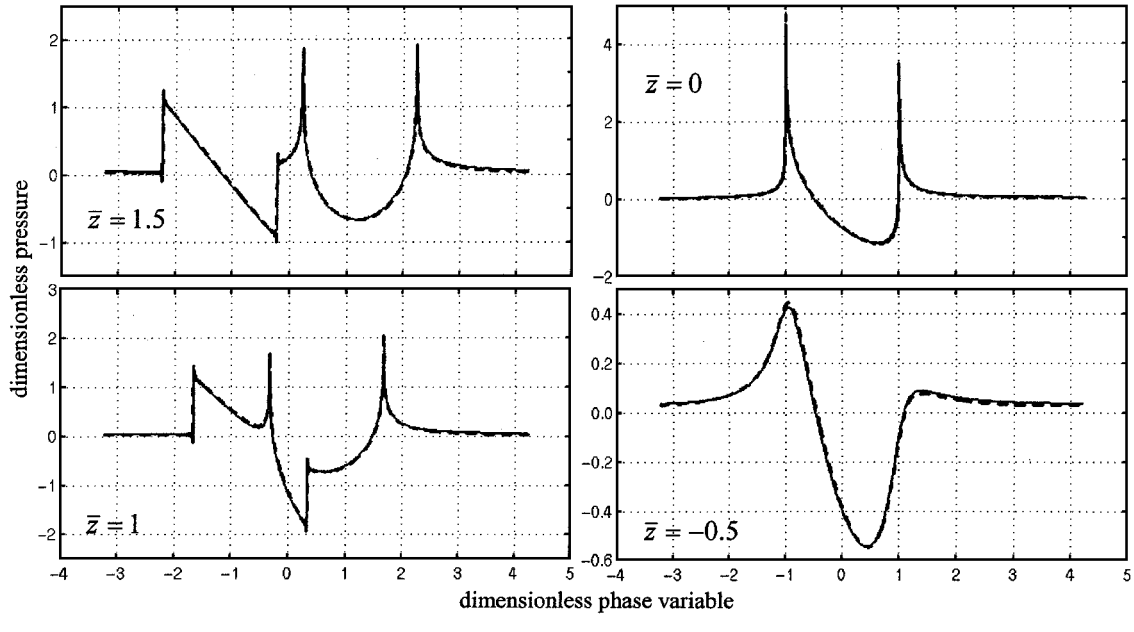

Fig. 4 Comparison between analytical (- - - -) and numerical (——) solutions in the linear case at $\bar{z} = 1.5$, 1, 0 (caustic), and − 0.5 (shadow zone).

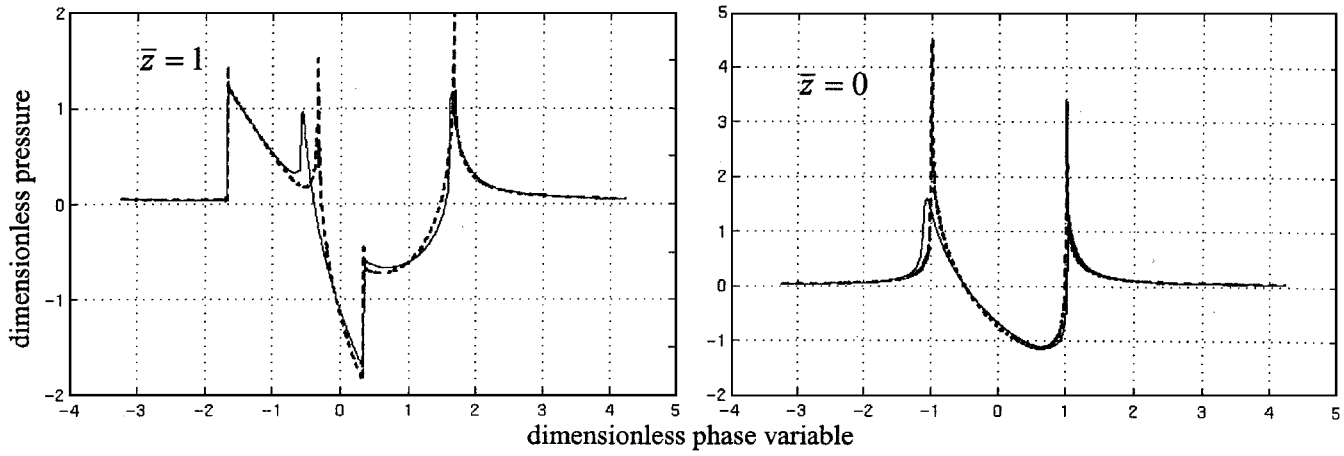

Fig. 5 Comparison between linear (– – –) and nonlinear ($\mu = 0.08$, ——) cases at $\bar{z} = 1$ and 0 (caustic).

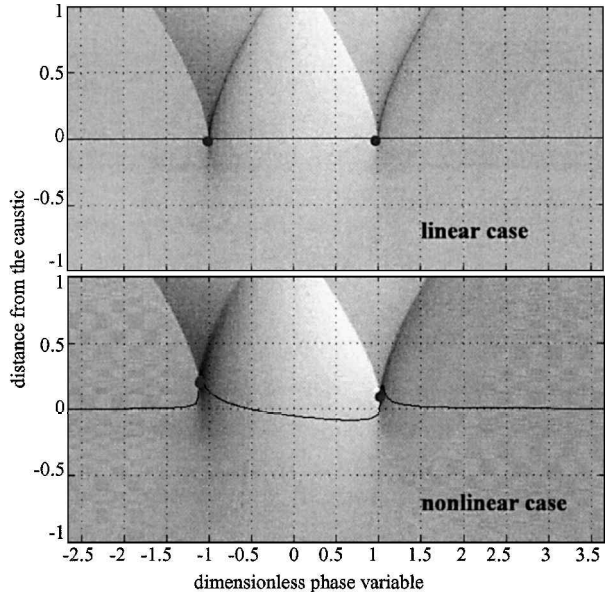

Fig. 6 Pressure gray plot in the linear and nonlinear ($\mu = 0.08$) cases; circles are the loci of the maximum amplitude for the bow and tail shocks.

identical. This shows that the numerical code is very robust, the converged solution being independent of the initial guess. Of course, the convergence requires many more iterations when the initial guess (such as the crenel) differs very much from the final solution, the optimum initial guess being the linear solution (roughly 400 iterations).

The third indirect validation is obtained by analyzing the influence of the number of frequencies on the signal amplitude. Figure 8 shows an enlargement of the first peak for four different cases ($\bar{z} = 0$ in the linear case, $\bar{z} = 0$ in the nonlinear case, $\bar{z} =$ the locus of the maximum pressure for the first peak, and $\bar{z} =$ the locus of the maximum pressure for the second peak) and three numbers of frequencies: 512 (solid line), 1024 (broken line), and 2048 (dotted line). The corresponding number of points in the z direction was equal to 1250, 3500, and 10,000, respectively.

In the linear case, on the caustic (Fig. 8a), the increase in the number of frequencies enhances the amplitude of the signal. (There is a 15% increase of the maximum amplitude using 2048 instead of 1024 frequencies.) This was expected because, for an infinite range of frequencies, we have to recover the theoretical infinite peak. In the linear case, there cannot be convergence for any positive $\bar{z}$.

In the nonlinear case, on the caustic (Fig. 8b), signal amplitude is independent of the number of frequencies, which shows the discretization is sufficient to converge to a bounded amplitude. That convergence is satisfied similarly at any distance from the caustic, in either the hyperbolic or the elliptical domain. However, the convergence turns out to be slower at the locus of maximum amplitude, where the first peak remains extremely sharp, even in the nonlinear case. There is an analogous phenomenon at the point of maximal amplification of the second shock of the N wave. Nevertheless, the amplitude of these maxima increases much more slowly than in the linear case. (There is only a 7% increase in the maximum amplitude using 2048 instead of 1024 frequencies.) We suspected that the point of maximum amplitude could correspond to a triple point, which is a singularity of the Tricomi equation, according to Tabak and Rosales.[25] However, this hypothesis is not acceptable because the maximum is located in the elliptical domain and, therefore, cannot correspond to the junction of three shock waves, which is necessarily in the hyperbolic region. Another, more convincing, explanation is that, at the locus of these points, solutions are regular but especially sharp and therefore, difficult to capture numerically despite the fine discretization (more than 20×10^6 points for the finest discretization). This situation is typical for acoustical problems because no such sharp peaks do occur in transonic aerodynamics.

Finally, we can conclude that convergence is satisfied almost everywhere but appears difficult to be reached at the locus of the maximum of pressure. Some studies are in progress to increase the capacities of the numerical code to check that point further.

The ultimate validation is to check Guiraud's scaling law.[1] Guiraud's scaling law is the only direct quantitative test in the nonlinear case. Indeed, it is an exact result, but only for incoming perfect step shock. Therefore, it seemed to us important to check our numerical algorithm vs this law. This is all the more important because Guiraud's scaling law is explicitly used in approximate solutions[8,15] for predicting sonic boom focusing.

The nonlinear Tricomi equation (1) and the boundary conditions (5–7) can be rewritten as

$$\frac{\partial^2 \Pi}{\partial Z^2} - Z\frac{\partial^2 \Pi}{\partial \Theta^2} + \frac{\partial^2}{\partial \Theta^2}\left(\frac{\Pi^2}{2}\right) = 0$$

$$\Pi(\Theta \to \pm\infty, Z) = \Pi(\Theta, Z \to -\infty) = 0$$

$$\Pi(\Theta, Z \to +\infty) = Z^{-\frac{1}{4}}\left\{\bar{F}\left[\mu^{\frac{6}{5}}\left(\Theta + \frac{2}{3}Z^{\frac{3}{2}}\right)\right] + \bar{G}\left[\mu^{\frac{6}{5}}\left(\Theta - \frac{2}{3}Z^{\frac{3}{2}}\right)\right]\right\} \tag{11}$$

using the following change of variables:

$$\bar{p}_a = \mu^{-\frac{1}{5}}\Pi, \qquad \bar{\tau} = \mu^{\frac{6}{5}}\Theta, \qquad \bar{z} = \mu^{\frac{4}{5}}Z \tag{12}$$

If the incoming wave is a step shock (invariant by phase dilatation), Eq. (11) and, therefore, its solution are obviously independent of μ.

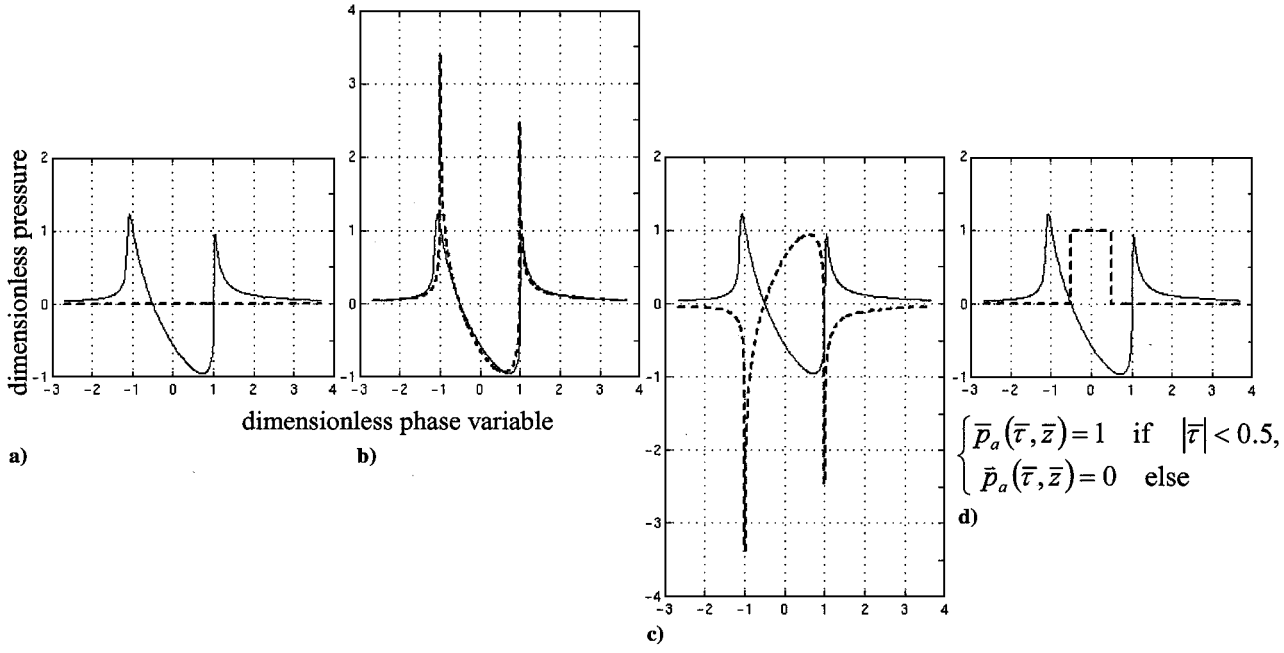

Fig. 7 Computed time signals ($\mu = 0.08$) at the caustic (——) independent of the initial guess (– – –): a) zero, b) linear solution, c) opposite of the linear solution, and d) crenel.

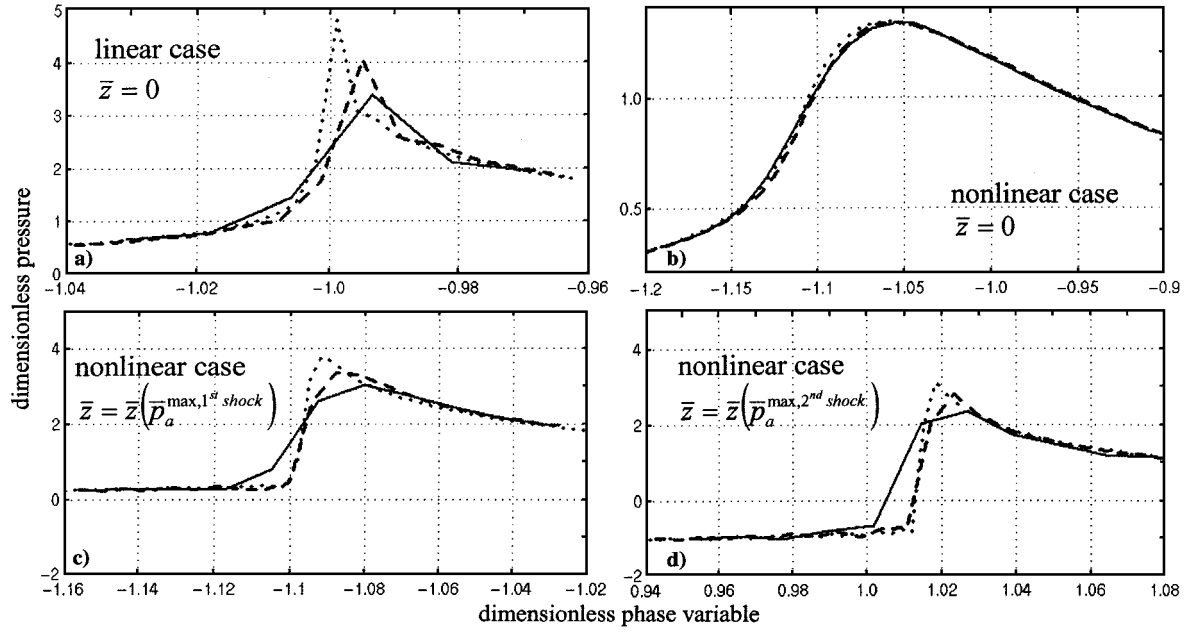

Fig. 8 Influence of the number of frequencies (——, 512; – – –, 1024; and · · · ·, 2048) on the convergence of the peak pressures: a) peak pressure at the caustic in the linear case, b) peak pressure at the caustic in the nonlinear case ($\mu = 0.08$), c) peak pressure in the nonlinear case ($\mu = 0.08$) at the locus of maximum amplitude, and d) peak pressure of the second maximum.

With a return to the original dimensionless variables, this implies that the pressure field around the caustic varies as $\mu^{-1/5}$. In particular, there exist constants C_G, $C_{G\tau}$, and C_{Gz} such that the maximum amplitude $\bar{p}_a^{\max}$ and its position $\bar{\tau}(\bar{p}_a^{\max})$ and $\bar{z}(\bar{p}_a^{\max})$ satisfy

$$\bar{p}_a^{\max} = C_G \mu^{-\frac{1}{5}}, \qquad \bar{\tau}\left(\bar{p}_a^{\max}\right) = C_{G\tau}\mu^{\frac{6}{5}}$$
$$\bar{z}\left(\bar{p}_a^{\max}\right) = C_{Gz}\mu^{\frac{4}{5}} \tag{13}$$

With a return to the physical variables, Guiraud's scaling law[1] means that the amplitude of a focused wave in the vicinity of a smooth caustic varies as power four-fifths of the amplitude of the incoming wave if this one is a step shock. There exists a similar scaling law for cusped caustics, but the power then is two-thirds instead of four-fifths.[21] Obviously, Guiraud's scaling law[1] is intrinsically nonlinear. Proving that our numerical scheme satisfies this law will give us a strong confidence in its validity in the nonlinear case.

The pseudospectral nature of our code requires the use of periodic incoming waves. Therefore, we cannot simulate a true step shock. However, in case of a periodic shock wave and a small μ, nonlinear effects are expected to affect almost exclusively the shock waves by limiting the amplitude of outgoing peaks in a small region of order $\mu^{6/5}$ for $\bar{\tau}$ and $\mu^{4/5}$ for $\bar{z}$. In this region, the behavior of the solution is expected to be similar to an isolated step shock. This property is used, for instance, by Gill and Seebass,[8] to determine approximate solutions for μ values such that their hodograph method does not enable them to locate shock waves. Therefore, Guiraud's scaling law[1] [Eq. (13)] is checked in Fig. 9 for two different types of periodic shock waves: a periodic saw-toothed wave (broken line) and a periodic pseudostep (solid line) with constant plateau values on the left- and right-hand sides of the shock. This last one is expected to

Table 1 Focusing due to acceleration in standard atmosphere

Acceleration, $m \cdot s^{-2}$	Mach	μ	$\bar{p}_a^{max}$	P_0, Pa	P^{max}, Pa	$\bar{z}(\bar{p}_a^{max})$	Boundary-layer thickness, m
			11.500 m				
0.2	1.161	0.0751	2.9047	51.5933	149.8631	0.1026	500.3414
0.4	1.1742	0.0746	2.8053	51.9724	145.7982	0.1037	484.4704
0.6	1.1881	0.0772	2.8635	52.0731	149.1113	0.1043	479.8086
0.8	1.2018	0.0793	2.8794	51.8124	149.1886	0.1009	479.1981
1	1.2149	0.0799	2.9219	52.9147	154.6115	0.1037	462.7679
			12.000 m				
0.2	1.1611	0.0689	2.8343	49.4604	140.1856	0.098	489.174
0.4	1.1745	0.0738	2.9534	48.8129	144.1640	0.102	498.4926
0.6	1.1887	0.075	2.8371	49.257	139.7470	0.1032	487.3308
0.8	1.2026	0.0764	2.792	49.9749	139.5299	0.1066	474.4114
1	1.216	0.0773	2.8671	50.4399	144.6162	0.1026	465.8065
			12.500 m				
0.2	1.1611	0.0728	2.9222	46.1063	134.7318	0.0992	523.8691
0.4	1.1747	0.0725	2.9063	47.4471	137.8955	0.1009	494.0023
0.6	1.1892	0.0759	2.9127	46.8411	136.4341	0.1026	501.0383
0.8	1.2034	0.0749	2.7785	47.0229	130.6531	0.0997	488.099
1	1.2172	0.073	2.8975	47.937	138.8975	0.997	465.1803

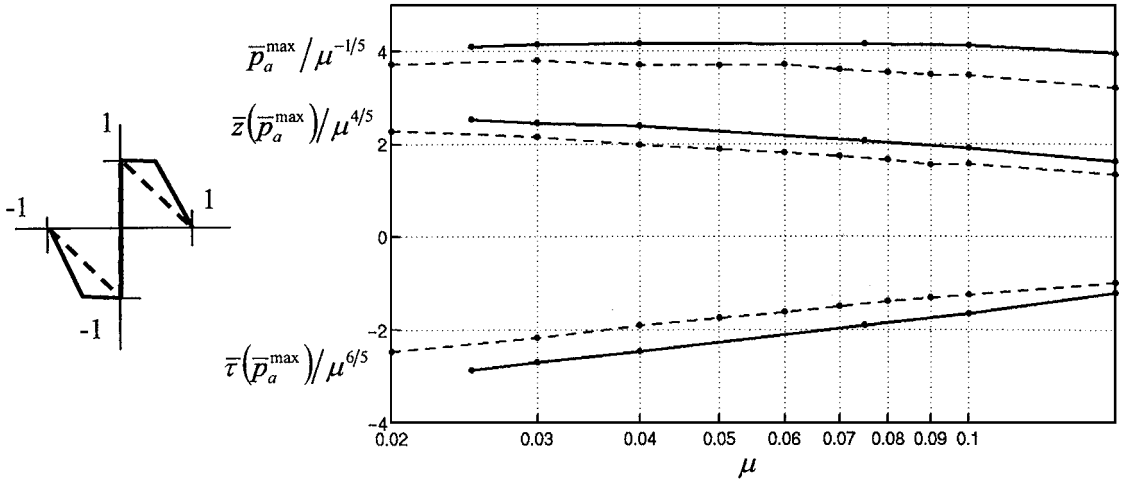

Fig. 9 Numerical check of Guiraud's scaling law[1] for a periodic saw-toothed function (– – –) and a pseudostep shock (——).

be closer to a true step shock and to better satisfy Guiraud's scaling law.

We notice in Fig. 9 that Guiraud's scaling law[1] is perfectly satisfied for the maximum pressure in case of a pseudostep shock (with a deviation from a constant value less than 4% for a one decade variation of μ). As expected, it is not as well satisfied for a saw-toothed wave, especially for the largest values of μ (deviation of 13%). Similar results can be observed for the maximum pressure on the caustic itself.[19] This confirms that the interaction between the shock wave itself and the nonconstant parts of the wave profile on each side is not completely negligible. This result disagrees with the assumptions of Gill and Seebass[8] and Plotkin[15] that it is possible to use Guiraud's scaling law[1] directly on the N wave to obtain the intensity of focusing.

For the position of this maximum, results are not so satisfying either for the distance from the caustic (deviation of 37%) or for the phase (deviation of 73%). Numerical simulations would rather indicate scaling laws of the form $\bar{\tau}(\bar{p}_a^{max}) = C_{G\tau}\mu^{0.8}$ and $\bar{z}(\bar{p}_a^{max}) = C_{Gz}\mu^{0.6}$, instead of Eq. (13). This deviation is probably related to the periodic character of the signal, which imposes strong constraints on the phase variable and does not enable it to vary as much as for an unconstrained true step shock. This again confirms that Guiraud's scaling law[1] is probably limited to pure step shocks, and its application to more realistic signals is questionable.

VI. Focusing of Concorde Sonic Boom

The numerical solver of the nonlinear Tricomi equation is now used to simulate the focusing of a Concorde sonic boom during its acceleration phase from Mach 1 to cruise at Mach 2. The complete simulation requires 1) computing the flowfield around the aircraft, 2) propagating the signal down to the ground according to the classical nonlinear geometrical theory, 3) determining the input data $\bar{F}$ and μ of the numerical code, and finally 4) executing the last one.

Sonic boom focusing is caused by the aircraft acceleration. Simulations are performed in the standard atmosphere,[19] for an aircraft flying horizontally with a constant acceleration, ranging from 0.2 to 1 ms^{-2}. Three different altitudes were examined, 11.5, 12, and 12.5 km. Only ground track simulations are investigated. The Mach numbers corresponding to the time of emission of the ray tangenting the caustic at the ground vary from 1.161 to 1.2172. The acoustical aircraft near field is estimated according to Whitham's function.[26] Ground parameters as given by geometrical acoustics vary little: The maximum overpressure of the incoming wave is between 46.1 and 52.9 Pa, and the dimensionless parameter μ is between 0.0698 and 0.0799, corresponding to a diffraction boundary thickness between 462 and 524 m (Table 1). The shape of the incoming wave is always similar. Therefore, we can conclude that acceleration and altitude have a very little influence on ground track focusing.

Let us consider now with more detailed results the case of an aircraft flying at 12 km with a 0.6-ms^{-2} acceleration. Then the incoming amplitude is 49.26 Pa, the dimensionless parameter μ is 0.0750, and the boundary-layer thickness is 487 m. The incoming signal (Fig. 10) has not reached its final N waveform and presents four shock waves, two bow shocks (emanating from the nose and from the leading edge of the wings), one very small intermediate shock, and finally the tail shock. The presence of the two bow shocks of comparable amplitudes leads to a more complex waveform

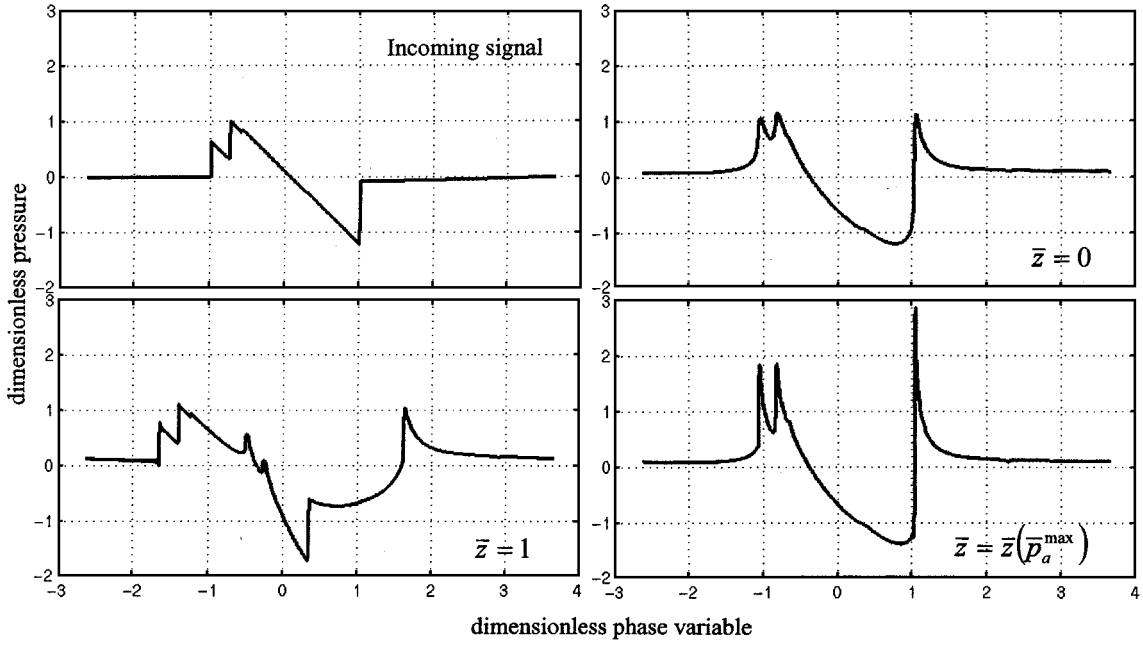

Fig. 10 Numerical simulation of Concorde sonic boom ground track focusing due to constant acceleration ($0.6\ \mathrm{ms}^{-2}$) and horizontal flight (altitude 12 kms) in standard atmosphere: incoming signal and dimensionless simulations at three different distances.

distortion, each incoming shock wave giving rise to an outgoing peak. In particular, the tail shock, with a larger amplitude, gives rise to the most amplified peak, contrarily to the N wave, where the highest peak emanates from the bow shock. Exactly at the caustic, there is a complex waveform with three peaks of almost equal amplitudes (Fig. 10). Such complex shapes could not be handled by the method of Plotkin[15] because it relies on Guiraud's scaling law,[1] which would be inapplicable here because the two bow shocks are sufficiently close to one another to interact strongly.

We can define an amplification coefficient (so-called focus factor by Wanner et al.[5]) as the ratio of the maximum pressure near the caustic to the amplitude of the incoming wave at a distance equal to one boundary-layer thickness from the geometrical caustic:

$$f = \frac{\bar{p}_a^{\max}}{\max[\bar{p}_a(\bar{z}=1)]} \tag{14}$$

Compared to the amplification coefficients used in the literature, this one is precisely defined by taking the reference incoming field at one boundary-layer thickness. For Concorde simulations (Fig. 10), $f = 2.84$, whereas for an N wave, $f = 3.5$. This would correspond to a maximum ground overpressure of 280 Pa (instead of 345 Pa for an N wave), taking into account the pressure doubling due to rigid ground reflection. Wanner et al.[5] give (not precisely defined) amplification factors ranging from 2 to 5, for different types of fighter aircraft and of maneuvers. Our simulations are well within that range. Also notice that the position of the maximum overpressure is shifted to 50 m from the geometrical caustic.

Finally, this numerical solver allows, on the one hand, locating and predicting precisely the maximum overpressure of a sonic boom focusing for any complex signal containing some shocks and, on the other hand, assessing the incoming wave shape to minimize this amplification.

The simulations clearly show that an efficient reduction in the amplitude of the focused boom is achievable by designing the aircraft so that the incoming wave does not reach an N waveform but rather displays several moderate shocks. Further minimization could be obtained, for instance, for an incoming signal having three bow shocks and two tail shocks. This opens a new way for minimizing sonic boom environmental impact, whereas previous studies have dealt only with minimization of primary boom for cruise flights.

VII. Conclusions

An original numerical method is presented for simulating sonic boom focusing by solving the nonlinear Tricomi equation. The numerical scheme has been validated by comparisons with exact solutions in the linear case and by tests of convergence and comparisons with Guiraud's scaling law[1] in the nonlinear case. As expected, nonlinear effects are shown to limit sharply the peak amplitude. These numerical simulations will be extended in the future to simulate lateral focusing. The aircraft acoustical near field will be given by CFD simulations instead of the approximate Whitham's function.[26] Nevertheless, the present results already show the amplitude of a focused boom could be reduced if the incoming signal is unstructured, with as many small shocks as possible.

References

[1] Guiraud, J.-P., "Acoustique Géométrique, Bruit Balistique des Avions Supersoniques et Focalisation," *Journal de Mécanique*, Vol. 4, 1965, pp. 215–267 (in French).

[2] Hayes, W. D., Haefeli, R. C., and Kulsrud, H. E., "Sonic Boom Propagation in a Stratified Atmosphere with Computer Program," NASA CR-1299, 1969.

[3] Berry, M. V., "Singularities in Waves and Rays," *Physics of Defects*, edited by R. Balian, M. Kleman, and J.-P., Poirier, North-Holland, Amsterdam, 1981, pp. 453–543.

[4] Buchal, R. N., and Keller, J. B., "Boundary Layer Problems in Diffraction Theory," *Communications on Pure and Applied Mathematics*, Vol. 13, 1960, pp. 85–114.

[5] Wanner, J.-C., Vallee, J., Vivier, C., and Thery, C., "Theoretical and Experimental Studies of the Focus of Sonic Booms," *Journal of the Acoustical Society of America*, Vol. 52, 1972, pp. 13–32.

[6] Sturtevant, B., and Kulkarny, V. A., "The Focusing of Weak Shock Waves," *Journal of Fluid Mechanics*, Vol. 73, 1976, pp. 651–671.

[7] Seebass, A. R., "Nonlinear Acoustic Behavior at a Caustic," *Third Conference on Sonic Boom Research*, NASA SP-255, 1971, pp. 87–120.

[8] Gill, P. M., and Seebass, A. R., "Nonlinear Acoustic Behavior at a Caustic: An Approximate Analytical Solution," AIAA Paper 73-1037, 1973.

[9] Seebass, A. R., Murman, E. M., and Krupp, J. A., "Finite Difference Calculation of the Behavior of a Discontinuous Signal Near a Caustic," *Third Conference on Sonic Boom Research*, NASA SP-255, 1971, pp. 361–371.

[10] Murman, E. M., and Cole, J. D., "Calculation of Plane Steady Transonic Flows," *AIAA Journal*, Vol. 9, No. 1, 1971, pp. 114–121.

[11] Yu, N. J., and Seebass, A. R., "Computational Procedures for Mixed Equations with Shock Waves, in Computational Methods in Nonlinear Mechanics," Texas Inst. for Computational Mechanics, 1974, pp. 499–508.

[12] Moretti, G., "Thoughts and Afterthoughts about Shock Computations," Polytechnical Inst., PIBAL Rept. 72-37, Brooklyn, NY, 1972.

[13] McDonald, B. E., and Kuperman, W. A., "Time Domain Formulation for Pulse Propagation Including Nonlinear Behavior at a Caustic," *Journal of the Acoustical Society of America*, Vol. 81, 1987, pp. 1406–1417.

[14]Zabolotskaya, E. A., and Khokhlov, R. V., "Quasi-Plane Waves in the Nonlinear Acoustics of Confined Beams," *Soviet Physics—Acoustics*, Vol. 15, 1969, pp. 35–40.
[15]Plotkin, K. J., "State of the Art of Sonic Boom Modeling," *Journal of the Acoustical Society of America*, Vol. 111, Pt. 2, 2002, pp. 530–536.
[16]Hayes, W. D., "Similarity Rules for Nonlinear Acoustic Propagation Through a Caustic," *Second Conference on Sonic Boom Research*, NASA SP-180, 1968, pp. 165–171.
[17]Coulouvrat, F., "Synthèse Bibliographique sur la Focalisation de la Détonation Balistique," Univ. Pierre et Marie Curie, Rapport Contrat Aérospatiale 96/065, Paris, 1997 (in French).
[18]Rosales, R. R., and Tabak, E. G., "Caustics of Weak Shock Waves," *Physics of Fluids*, Vol. 10, 1997, pp. 206–222.
[19]Auger, T., "Modélisation et Simulation Numérique de la Focalisation d'Ondes de Choc Acoustiques en Milieu en Mouvement. Application à la Focalisation du Bang Sonique en Accélération," Dissertation, Univ. Pierre et Marie Curie, Paris, 2001 (in French).
[20]Abramowitz, M., and Stegun, I., *Handbook of Mathematical Functions*, Dover, New York, 1965, p. 448.
[21]Coulouvrat, F., "Focusing of Weak Acoustic Shock Waves at a Caustic Cusp," *Wave Motion,* Vol. 32, 2000, pp. 233–245.
[22]Coulouvrat, F., "Sonic Boom in the Shadow Zone: A Geometrical Theory of Diffraction," *Journal of the Acoustical Society of America*, Vol. 111, Pt. 2, 2002, pp. 499–508.
[23]Frøysa, K.-E., Tjøtta, J. N., and Berntsen, J., "Finite Amplitude Effects in Sound Beams. Pure Tone and Pulsed Excitation," *Advanced in Nonlinear Acoustics*, edited by H. Hobæk, World Scientific, Singapore, 1993, pp. 233–238.
[24]McDonald, B. E., and Ambrosiano, J., "High-Order Upwind Flux Methods for Scalar Hyperbolic Conservation Laws," *Journal of Computational Physics*, Vol. 56, 1984, pp. 448–460.
[25]Tabak, G. E., and Rosales, R. R., "Focusing of Weak Shock Waves and the Von Neumann Paradox of Oblique Shock Reflection," *Physics of Fluids*, Vol. 6, 1994, pp. 1874–1892.
[26]Whitham, G. B., "The Flow Pattern of a Supersonic Projectile," *Communications in Pure and Applied Mathematics*, Vol. 5, 1952, pp. 301–348.

P. J. Morris
Associate Editor